This paper considers elastic shell elements. They move under pressure. The type of dependence of displacement on pressure is called the elastic characteristic of the element. The object of this study is shell elements with a complex surface shape, consisting of composite materials of the "metal-metal" type. The composite is a metal shell with reinforcing fiber made of another metal material. The form of reinforcement is different. The task to be solved is to determine the elastic characteristics of the shell elements depending on the geometric parameters, as well as the mechanical values of the shell at its various points and in different directions. To this end, algorithms were built for calculating mechanical quantities depending on the percentage of the fiber and the shell matrix. It was required to derive a system of equations for determining the displacements and internal forces in the element depending on the geometric and mechanical parameters. A numerical calculation of shell elastic elements was performed and a comparison of the results of analytical calculation according to the algorithm developed in this work and experimental data was performed. The match between these results is 99.8–100 %. The characteristics of the shell elements were determined depending on the type of reinforcing fiber and matrix, on the geometric parameters, and the type of reinforcement of the shell. These studies make it possible to design shell elements with specified characteristics and predefined sensitivity

Keywords: corrugated shell membrane, elastic static characteristic, composite materials, mechanical characteristics of reinforced shells

UDC 624.9
DOI: 10.15587/1729-4061.2022.269399

DETERMINING STATIC CHARACTERISTICS OF CORRUGATED SHELL ELEMENTS MADE FROM COMPOSITE MATERIALS

Irina Polyakova
PhD*
Raikhan Imambayeva
PhD*
Bakyt Aubakirova
Corresponding author
PhD*
E-mail: aubakirova.baxyt@mail.ru
Nazym Shogelova
Master of Technical Sciences*
Yevgeniya Glyzno
Master of Technical Sciences, Assistant Professor*
Aigerim Zhumagulova
Master of Technical Sciences *
*Faculty of General Construction
International Educational Corporation, Campus "Kazakh Head of Architecture and Civil Engineering Academy"
Ryskulbekova str., 28, Almaty, Republic of Kazakhstan, 050050

Received date 14.10.2022
Accepted date 16.12.2022
Published date 30.12.2022

How to Cite: *Polyakova, I., Imambayeva, R., Aubakirova, B., Shogelova, N., Glyzno, Y., Zhumagulova, A. (2022). Determining static characteristics of corrugated shell elements made from composite materials. Eastern-European Journal of Enterprise Technologies, 6 (7 (120)), 63–76. doi: https://doi.org/10.15587/1729-4061.2022.269399*

1. Introduction

In modern construction, as well as mechanical engineering, instrumentation, various types of measuring instruments and sensors are used. The most important functional unit of such devices are elastic sensitive elements, the main working property of which is the ability to significantly deform under load. As a rule, these deformations are elastic, and after removing the load, the element restores its size. Every year, shell elastic elements (SEE) are increasingly used as elastic elements, specifically thin-walled corrugated shells of growth such as, for example, corrugated membranes.

The geometric shape of elastic elements can be very diverse and depends on the purpose and conditions of their operation.

Manometric elastic elements loaded during operation by pressure are considered. This pressure acts on an elastic element, for example, a corrugated membrane, the center of which executes a linear displacement. This displacement is transmitted by means of a transfer mechanism to the arrow of the device. In this case, the membrane serves to convert pressure into displacement.

A corrugated shell membrane differs from a flat membrane by the presence of concentric waves. The properties of a corrugated membrane depend on its profile. The elastic characteristic at different profiles can be linear, attenuated, or increasing in pressure. In this respect, corrugated membranes have an advantage over other types of gauge elastic elements (bellows, tubular springs), the elastic characteristics of which are close to linear [1]. With the help of corrugated membranes, usually equipped with a rigid center, the tasks of measuring displacement, linearly or nonlinearly associated with pressure, are solved. The advantage of corrugated membranes over flat membranes is manifested in the fact that at the same pressure, the corrugated membrane makes large displacements, and, therefore, has greater sensitivity than a flat one.

The accelerated development of technology imposes increased requirements on the materials from which structures and their elements are made. One of the most important requirements is to minimize the mass of structural elements while maintaining their performance characteristics. This is most fully met by composite materials developed only relatively recently, but, despite this, which are increasingly used in various fields of technology.

Previously, the work of elastic shells made of monomaterials, or smooth shells, was studied. Research into the static characteristics of corrugated shells made of composite materials is relevant because it will make it possible to design shell elements with specified parameters, up to a decrease in their mass, which leads to a decrease in the weight of building structures.

2. Literature review and problem statement

Elastic elements are usually thin-walled shells of rotation, in particular, corrugated, the meridional cross-section of which is a wave-like curve. Such shells can be prepared by applying concentric ring corrugations of arbitrary shape to any surface of rotation, called the initial or main one. Work [1] considers elastic elements in the form of thin-walled shells of rotation with the shape of a meridian in the form of corrugations of various depths but consisting of monomaterials. Such elastic elements have the same physical and mechanical properties in all directions. However, stresses in elastic elements are determined only at static loads. Paper [2] considers the theory of calculation of multilayer shells made of isotropic materials. The shells are represented as smooth, and anisotropy is caused by a combination of different materials. However, shells with an arbitrary meridian shape are not considered. Paper [3] considered the definition of elastic permanent, taking into account the heterogeneity of the shells caused by uneven reinforcement. Clarified values of such characteristics are used in research. In work [4], the application of finite element methods for the calculation of a thin two-layer conical shell under the action of a uniformly distributed load using an axisymmetric finite element is outlined. The discrepancy between the results of the study of the proposed mathematical model and the available results of calculations according to analytical formulas for thin two-layer conical shells does not exceed 9.3 %. From a mathematical point of view, the finite element method is widely implemented in the calculation of building structures. But taking into account the uneven distribution of elastic characteristics in the calculation of heterogeneous corrugated shells will be very difficult to reflect when filling in the initial data, which makes this method difficult. Study [5] touches upon the issue of calculating multilayer structures by type of layered plates and shells. The authors analyzed existing approaches in the field of calculating layered plates and shells. It is established that the calculation of multilayer structures is considered using two main methods: the theory of elasticity and the methods of mechanics of composite materials. The isotropic, anisotropic, and orthotropic structures of plates and shells, which obeys Hooke's law, were considered. The choice of calculation method depends on the composition of the multilayer structure, the rigidity of the middle layer, and the diversity of all layers. Studies of the stress-strain state and the distribution of forces between the components of multilayer structures in the above calculations show that basically the deformation standing is described by Hooke's generalized law. An important factor is to take into account the general anisotropy of the structure and the work of the middle layer in the layered structure. However, shells with a complex meridian shape and shells with anisotropy caused by uneven reinforcement were not considered. Paper [6] discusses the same constructions as in the previous work but uses the SCAD (RF) program. A comparison of theoretical and computer calculations is given. For the same reasons that were indicated in the finite element calculation (FEM) method, this method is undesirable to use in the calculation of SEE. Study [7] considers the determination of proper oscillations of cylindrical shells of composites. However, composites are taken as various combinations of plastic materials, not matrix-reinforcing fiber combinations. In that work, the static characteristics of the shells were also not determined. Paper [8] considers various types of composites for use in building structures but without the calculation of specific structural elements for static effects. Work [9] formulates the initial-boundary problem of viscoelastic bending of cylindrical round shells transversely reinforced on equidistant surfaces. Instantaneous elastic-plastic deformation of the components of the shell is described by the basic equations of the theory of plastic flow with isotropic hardening. However, the dynamics of rotation shells made of composite materials are not considered. In [10], the multilayer shell is considered, and stresses and deformations are determined. However, the anisotropy of such shells is caused by different materials of the layers, and not by reinforcing fibers. Study [11] considers the tensile forces of the toroidal shell caused by pressure and rotation, and their effect on their own oscillations. However, dynamic forces are not taken into account and heterogeneous shells are not considered. In [12], the shells of rotation with a complex shape of the meridian on dynamic effects were considered, while the shell material was taken to be homogeneous, from a monomaterial. Study [13] reports a method for the formation of structural systems from wavy shells using a special complex material consisting of regular transformable shell elements bounded by spatial quadrangles. These structures are not elastic sensitive elements. Paper [14] considers a variant of the rotation shell in the form of a closed round cylindrical shell, which is often used in the practice of designing civil, energy, and other industrial structures. The peculiarity of the shell in question is in its material. It manifests a double anisotropy depending on the ambient temperature. Work [15] describes the tests of a cylindrical shell with physical and geometric nonlinearity. An approximate solution method is proposed, and its accuracy is determined. In [16], corrugated cylindrical shells with arbitrary boundary conditions. The influence of basic geometry parameters on the dynamic characteristics of corrugated shells is considered. However, static characteristics have not been studied. In [17], the geometry of spherical shells with corrugated edges, the wave-like perturbation of which is controlled by the corresponding equations and parameters, was considered. A simple example is given for pressure loading, to demonstrate the change in the properties of the structure due to the corrugated form. But the materials of the shell were taken to be homogeneous. In [18], spiral corrugation in an isotropic cylindrical shell was considered. This fact changes the isotropy of the structure. The design space of anisotropy is used to differentiate the effect of geometric parameters on the stiffness of spiral-corrugated cylindrical shells. In this case, the rotation shells were not considered. In [19], round and spiral-corrugated cylindrical shells were considered. The maximum von Mises stresses in wavy shells vary considerably compared to similar stresses in round shells. Rotation shells have not been studied. In [20], corrugated shells of monomaterials are considered, a method

for calculating such shells has been developed. The authors considered such a shell as a test case for determining the accuracy of the results. However, anisotropic shells made of composite materials are not considered in [20]. After analyzing the scientific literature, it becomes obvious that the task of determining the static elastic characteristics of shell corrugated elements from composite materials is very relevant and is of interest both scientifically and in the manufacture of these elements.

3. The aim and objectives of the study

The purpose of this study is to develop a method for calculating the performance characteristics (elastic characteristics, static sensitivity) of corrugated shell elastic elements made of composite materials. This theoretical study will make it possible to design elastic shell elements with specified static characteristics, as well as to improve the accuracy of the measured values.

To accomplish the aim, the following tasks have been set:

– to build an estimation scheme of the elastic element as a shell of rotation under deformation and equilibrium equations;

– to derive equations for determining the displacements and forces in corrugated shell elastic elements;

– to reduce the system of equations to a dimensionless form and determine the vector of the state;

– to determine the displacements, forces, and stresses in corrugated elastic elements.

4. The study materials and methods

The object of our study is shell elements with a complex surface shape and consisting of composite materials of the "metal-metal" type. The composite is a metal shell with reinforcing fiber made of another metal material.

The main hypothesis of the study assumes that when calculating the shells of rotation, the Kirchhoff Love's hypotheses hold. The use of this model in the first approximation makes it possible to achieve sufficient accuracy in solving a number of practical tasks. However, in this case, this scheme is not complete enough since we are talking about a shell of composite materials. Such shells are heterogeneous, anisotropic elastic systems. The presence of reinforcement, the combination of materials with various modulus of elasticity determines the features of the properties of structures, in particular, deformation. So, when bending such shells, shear compliance is of great importance in deformation, so here it is impossible to neglect the deformations corresponding to the tangential stresses along the normal. With respect to the layer package as a whole, the direct normals hypothesis is no longer acceptable. This applies to all shells of composite materials with a binder having relatively low shear stiffness. Therefore, in addition to the "classical" deformations, we introduce shear deformations associated with transverse forces.

Assumptions – shells with a relatively small amplitude of corrugation are considered. This circumstance is dictated by the technology of manufacturing elastic elements.

The main lines of curvature of the shells of rotation are meridians and parallels. These lines are taken as curvilinear coordinates. The position of point *N* (Fig. 1) on the median surface is characterized by two parameters (coordinates): the angle φ and the distance *s*.

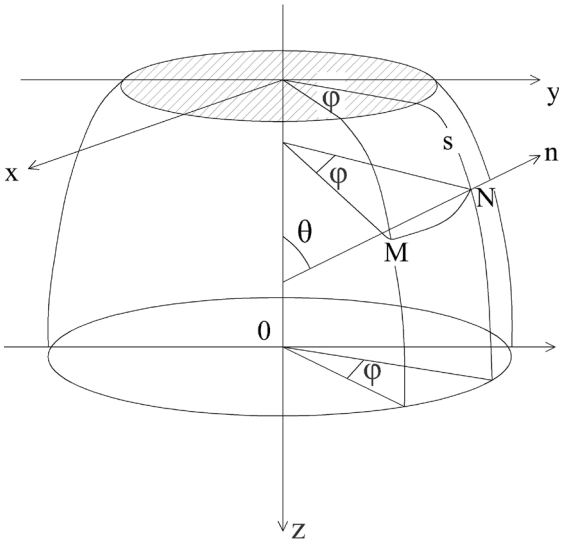

Fig. 1. Estimation scheme of deformed elastic shell element

The angle φ determines the position of the meridional plane in which a given point is located. The distance *s* is equal to the length of the arc of the meridian from some starting point to point *N*. The angle between the normal to the median surface of the shell and the axis of its symmetry is indicated by θ.

Fig. 2 shows an estimation scheme of an undeformed element.

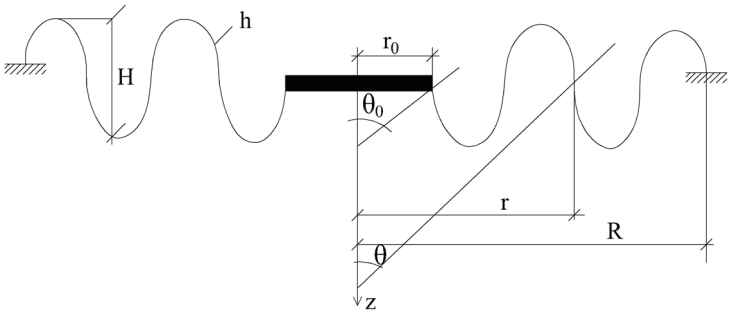

Fig. 2. Estimation scheme of an undeformed elastic element

Fig. 2 has the following designations: *H* - the amplitude of the corrugation, *h* – the thickness of the shell, *R* – the outer radius of the shell, *r* – the current radius of the shell, r_0 – the radius of the rigid center, θ_0 – the angle between the normal and the *z* axis at $r=r_0$, θ – the angle between the normal and z-axis at $r=r_0$.

Two static models of corrugated shell elements, described in Table 1, were considered.

Three variants of the structures of corrugated shell elastic elements from composite materials are considered (Fig. 3, *a–c*). The choice of these options is dictated by the technology of manufacturing shell elements and the peculiarities of their work as elastic sensitive elements.

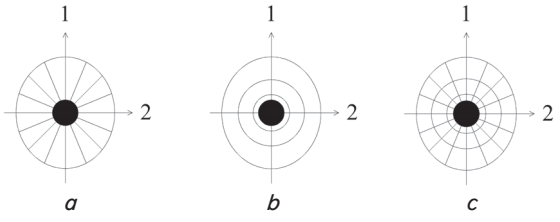

Fig. 3. Variants of the structure of corrugated shell elastic elements made of composite materials: *a* — unidirectional with a radial arrangement of fibers; *b* — unidirectional with an annular arrangement of fibers; *c* — orthogonally reinforced

Table 1

Types of element models

Static Model Designation (SM)	Nature of deformation	Types of accepted theories and hypotheses	Scope of the model
SM-1	Low deflection without consideration of transverse shear	Linear theory of thin shells and the Kirchhoff-Love conjecture	GOUEKM with a matrix with a sufficiently high shear stiffness
SM-2	Small deflections due to transverse shear	Linear theory of thin shells and the Tymoshenko-type hypothesis	GOECM with a matrix with relatively low shear stiffness

As a coordinate surface, the median surface is chosen, dividing the thickness of the shell into two equal parts. Let's refer it to curvilinear orthogonal coordinates directed so that at each point of the shell the directions equivalent in terms of physical and mathematical properties coincide with them. The values of the mechanical characteristics at each point of the shell will depend on the concentration of the reinforcing fiber at each point:

$$E_1 = E_B\psi(r_0)\frac{r_0}{r} + E_M\left[1-\psi(r_0)\frac{r_0}{r}\right], \quad (1)$$

$$E_2 = \frac{E_B E_M}{E_B\left[1-\psi(r_0)\right] + E_M\psi(r_0)\frac{r_0}{r}}, \quad (2)$$

where E_1 is the modulus of elasticity in the direction of reinforcing fibers, and E_2 is the modulus of elasticity in the direction perpendicular to the reinforcing fibers, E_B is the modulus of elasticity of the fiber material, E_M is the modulus of elasticity of the matrix material, ψ is the volume content (concentration) of the fiber in the shell.

The Poisson coefficients and shear moduli are calculated as follows:

$$v_1 = \psi_B v_B + \psi_M v_M, \quad (3)$$

$$\nu_2 = \frac{\nu_1 E_2}{E_1}, \quad (4)$$

$$G_{12} = G_{21} = \frac{G_B G_M}{\psi_B G_M + (1-\psi_B)G_B}. \quad (5)$$

Here, ν_1 is the Poisson coefficient in the direction of the reinforcing fibers, ν_2 is the Poisson coefficient in the direction perpendicular to the reinforcing fibers, G_{12} is the shear modulus of the composite.

Tables 2, 3 give the values of these constants for different materials.

Table 2

Samples of matrix materials

No.	Material	Modulus of elasticity E (MPa)	Poisson's coefficient ν
1	Magnesium	43,600	0.42
2	Copper	112,000	0.34
3	Aluminum	72,000	0.31

Table 3

Samples of fiber materials

No.	Material	Modulus of elasticity E (MPa)	Poisson's coefficient ν
1	Boron	400,000	0.42
2	Steel	200,000	0.31
3	Aluminum	72,000	0.31

The elastic characteristic is the dependence between the linear axial displacement Uz of the rigid center of the elastic shell element and the load p. The elastic characteristic of the element can be linear and nonlinear: increasing (soft) or decreasing (hard) (Fig. 4) [1].

If the characteristic of the elastic element is linear, then the stiffness K is the ratio of the load to the corresponding displacement.

$$K=p/U_z; \quad (6)$$

and sensitivity S is the ratio of displacement to the load that caused it:

$$S=1/K=S=U_z/p. \quad (7)$$

The stiffness and sensitivity of an elastic element with a nonlinear characteristic vary depending on the deflection and are determined as follows:

$$K=\Delta p/\Delta U_z;\ S=\Delta U_z/\Delta p. \quad (8)$$

As can be seen from (8), sensitivity and stiffness are reciprocal quantities.

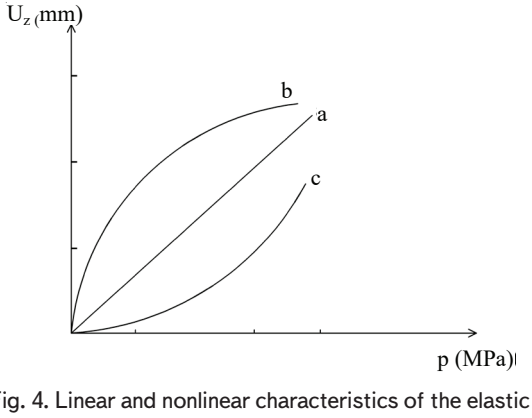

Fig. 4. Linear and nonlinear characteristics of the elastic element: *a* — linear; *b* — decreasing (soft); *c* — ascending (hard)

5. Results of the development of a methodology for determining the static characteristics of elastic shells

5. 1. Justification of the estimation scheme

The elastic element is considered as a shell of rotation. The calculation scheme for deriving equilibrium equations

is presented in Fig. 5, *a–c*. One of the equilibrium equations can be drawn up in integral form - this is the sum of the projections on the axis of symmetry of the forces applied to the final section of the shell (Fig. 5, *a, b*).

$$\left(N_1 \sin\theta - Q\cos\theta\right)2\pi r = F(s), \tag{9}$$

where $F(s)$ is the total axial load on the allocated part of the shell. The value of $F(s)$ consists of the axial load p_0 on the upper edge of the shell and the projections on the axis of loads q_1 and q_n distributed over the surface of the section.

$$F_s = Q\cdot 2\pi r = p_0\pi r_0^2 + \int_{S_0}^{S}\left(q_n\cos\theta - q_1\sin\theta\right)2\pi r ds, \tag{10}$$

$$\frac{d}{ds}\left(Q_Z\cdot 2\pi r\right) = \left(q_n\cos\theta - q_1\sin\theta\right)2\pi r,$$

$$\frac{d}{ds}\left(Q_Z\cdot r\right) = \left(q_n\cos\theta - q_1\sin\theta\right)r.$$

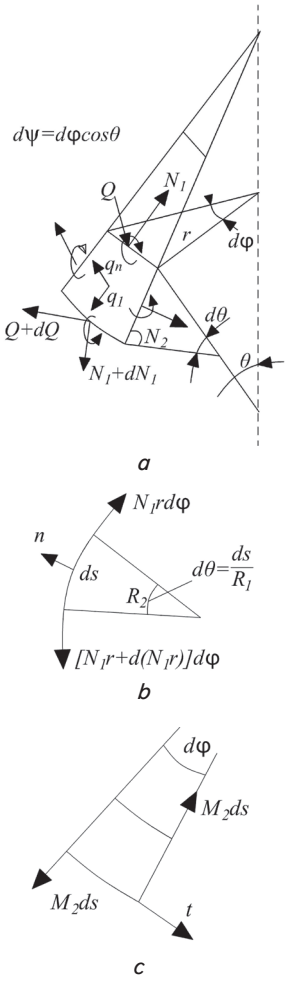

Fig. 5. Estimation scheme of the shell element: *a* — fragment of the shell element; *b* — projection of forces on the axis of symmetry; *c* — projection of forces in a cross-section perpendicular to the meridian

When calculating the shells of rotation, it is convenient, along with the projections N_1 and Q, to determine the forces in the cross-section normal to the meridian. Consider the projections of these forces on the direction of the axis of symmetry of the shell (Fig. 5, *b*) and on the direction of the normal to the axis (Fig. 5, *c*). The axial component of the force is equal in cross-section to $[F(s)/2\pi r]$, and normal to the symmetry axis, $Q_r=N_1\cos\theta+Q\sin\theta$; the component Q is called the spacer force [1, 2].

5. 2. Derivation of equations for determining displacements and forces in corrugated shell elastic elements

The equilibrium of the shell element, distinguished by two meridional sections and two sections normal to the meridian (Fig. 5, *a*) was considered. For the element of a symmetrically loaded shell, three non-identical equilibrium equations can be drawn up: two equations of projections on any directions lying in the meridional plane, and one equation of moments with respect to the axis normal to this plane. The sum of the projections of forces on the direction of the normal to the element is compiled. The equation of equilibrium includes the projection of the external load $q_n rd\phi ds$ ($rd\phi ds$ – the area of the element), the difference in the values of the transverse forces applied to the lower and upper faces of the element, $d(Q_1 r)d\phi$, as well as projections to the normal of the forces applied to the element N_1 and N_2. As can be seen from Fig. 5, *b*, the projection on the normal *n* of the forces N_1 with an accuracy of small higher order is $N_1 rd\varphi ds/R_1$.

Similarly, considering the normal to the meridian cross-section of the element, the projection to the normal of forces N_2 is equal to $N_1 rd\phi ds/R_2$.

Thus, the sum of the projections of all forces on the direction of the normal is:

$$d\left(Q_1 r\right)d\varphi - N_1 rd\varphi\frac{ds}{R_1} - N_2 rd\varphi\frac{ds}{R_2} + q_n rd\varphi ds = 0,$$

or, after reduction by $rd\varphi ds$,

$$\frac{1}{r}\frac{d}{ds}\left(Q_1 r\right) - \frac{N_1}{R_1} - \frac{N_2}{R_2} + q_n = 0. \tag{11}$$

The equation of moments of the forces with respect to the tangent *t* to the parallel passing through the lower face of the element.

$$\left(M_1 + dM_1\right)\left(r + dr\right)d\varphi - M_1 rd\varphi = d\left(M_1 r\right)d\varphi,$$

where M_1 is the angular momentum applied to the upper face of the transverse force $Qrd\phi ds$, as well as the projection of the moments $M_2 ds$ applied to the side faces. This equation includes the difference between the moments M_1 applied to the lower and upper faces of the element.

In order to calculate these three projections, the moments are depicted as vectors (Fig. 5, *c*). It was established that the angle between these vectors $d\psi=(rd\phi/r\cos\theta)=d\phi\cos\theta$. Therefore, the projection of vectors on the *t* direction:

$$-M_2 dsd\psi = -M_2 dsd\varphi\cos\theta.$$

The moment relative to *t* of the distributed loads is of a small higher order. So, the equation of moments is:

$$d\left(M_1 r\right)d\varphi - M_2 dsd\varphi\cos\theta - Q_1 rd\varphi ds = 0,$$

or, after reduction by $rd\phi ds$,

$$\frac{1}{r}\frac{d}{ds}(M_1 r)-M_2\frac{\cos\theta}{r}-Q_1=0. \quad (12)$$

In addition to the equations of equilibrium (11), (12), it is also possible to draw up a condition of equality to zero the sum of projections on the direction of the meridian of all forces applied to the element (Fig. 1). This equation is:

$$d(N_1 r)d\varphi-N_2 ds d\psi+Qrd\varphi d\theta+q_1 rd\varphi ds=0,$$

where the minor of higher orders are omitted. After reduction by $rd\phi ds$ and substitution

$$\frac{d\psi}{d\varphi}=\cos\theta,\frac{d\theta}{ds}=\frac{1}{R_1},$$

we obtain

$$\frac{1}{r}\frac{d}{ds}(N_1 r)-\frac{\cos\theta}{r}N_2+\frac{Q}{R_1}+q_1=0,. \quad (13)$$

$$\frac{du_r}{ds}=\varepsilon_1\cos\theta-\vartheta\sin\theta, \quad (14)$$

$$\frac{du_z}{ds}=\varepsilon_1\sin\theta+\vartheta\cos\theta. \quad (15)$$

We expressed the elongation of the ring fiber $\varepsilon_2=u_r/r$ through the intensity force N_2:

$$N_2=\frac{E_2 h}{1-\nu_1\nu_2}\left(\varepsilon_2+\frac{E_1}{E_2}\nu_2\varepsilon_1\right)=$$
$$=c_2\left(\varepsilon_2+\frac{E_1}{E_2}\nu_2\varepsilon_1\right)\to\varepsilon_2\frac{N_2}{c_2}-\frac{E_1}{E_2}\nu_2\varepsilon_1. \quad (16)$$

After substituting this value into an expression for N_1:

$$N_1=\frac{E_2 h}{1-\nu_1\nu_2}\left(\varepsilon_1+\frac{E_2}{E_1}\nu_1\varepsilon_2\right)=c_1\left(\varepsilon_1+\frac{E_2}{E_1}\nu_1\varepsilon_2\right)=$$
$$=c_1\left(\varepsilon_1+\frac{E_2}{E_1}\nu_1\left(\frac{N_2}{c_2}-\frac{E_1}{E_2}\nu_2\varepsilon_1\right)\right)=$$
$$=c_1\left(\varepsilon_1+\frac{E_2}{E_1}\nu_1\frac{N_2}{c_2}-\nu_1\nu_2\varepsilon_1\right)=$$
$$=c_1\varepsilon_1+\frac{c_1}{c_2}\frac{E_2}{E_1}\nu_1 N_2-c_1\nu_1\nu_2\varepsilon_1. \quad (17)$$

Substituting N_2 into this expression, we obtained:

$$N_1=c_1\varepsilon_1+\frac{c_1}{c_2}\frac{E_2}{E_1}\nu_1 c_2\left(\varepsilon_2+\frac{E_1}{E_2}\nu_2\varepsilon_1\right)-c_1\nu_1\nu_2\varepsilon_1=$$
$$=c_1\varepsilon_1+c_1\frac{E_2}{E_1}\nu_1\varepsilon_2+c_1\frac{E_2}{E_1}\nu_1\frac{E_1}{E_2}\nu_2\varepsilon_1-c_1\nu_1\nu_2\varepsilon_1=$$
$$=c_1\varepsilon_1 c_1\frac{E_2}{E_1}\nu_1\varepsilon_2+c_1\nu_1\nu_2\varepsilon_1-c_1\nu_1\nu_2\varepsilon_1=$$
$$=c_1\varepsilon_1+c_1\frac{E_2}{E_1}\nu_1\varepsilon_2. \quad (18)$$

We expressed from the last expression ε_1:

$$\varepsilon_1=\frac{N_1}{c_1}-\frac{E_2}{E_1}\nu_1\varepsilon_2=\left|\varepsilon_2=\frac{u_r}{r}\right|=\frac{N_1}{c_1}-\frac{E_2}{E_1}\nu_1\frac{u_r}{r}. \quad (19)$$

Considering that $N_1=Q_z\sin\theta+Q_r\cos\theta$, we obtained

$$\varepsilon_1=\frac{N_1}{c_1}-\nu_1\frac{E_2}{E_1}\frac{u_r}{r}=$$
$$=\frac{1-\nu_1\nu_2}{E_1 h}(Q_z\sin\theta+Q_r\cos\theta)-\nu_1\frac{E_2}{E_1}\frac{u_r}{r}, \quad (20)$$

or, what is the same:

$$\varepsilon_1=\frac{1-\nu_1\nu_2}{E_1 h}Q_z\sin\theta+\frac{1-\nu_1\nu_2}{E_1 h}Q_r\cos\theta-\nu_1\frac{E_2}{E_1}\frac{u_r}{r}. \quad (21)$$

Substituting this expression in (6) and (7), we obtained:

$$\frac{du_r}{ds}=\frac{1-\nu_1\nu_2}{E_1 h}Q_z\sin\theta+\frac{1-\nu_1\nu_2}{E_1 h}Q_r\cos^2\theta-$$
$$-\nu_1\frac{E_2}{E_1}\cos\theta\frac{u_r}{r}-\vartheta\sin\theta, \quad (22)$$

$$\frac{du_z}{ds}=\frac{1-\nu_1\nu_2}{E_1 h}Q_z\sin^2\theta+\frac{1-\nu_1\nu_2}{E_1 h}Q_r\sin\theta\cos\theta-$$
$$-\nu_1\frac{E_2}{E_1}\sin\theta\frac{u_r}{r}+\vartheta\cos\theta. \quad (23)$$

It is known that

$$K_1=\frac{d\vartheta}{ds},\quad K_2=\frac{\cos\theta}{r}\vartheta.$$

Substituting these values in

$$M_1=D_1\left(K_1=\frac{E_2}{E_1}\nu_1 K_2\right),$$

we obtained

$$M_1=D_1\left(\frac{d\vartheta}{ds}+\frac{E_2}{E_1}\nu_1\frac{\cos\theta}{r}\vartheta\right). \quad (24)$$

After the conversion, we have

$$\frac{d\vartheta}{ds}=\frac{M_1}{D_1}+\frac{E_2}{E_1}\nu_1\frac{\cos\theta}{r}\vartheta, \quad (25)$$

or, finally:

$$\frac{d\vartheta}{ds}=\frac{12(1-\nu_1\nu_2)}{E_1 h^3}M_1-\frac{E_2}{E_1}\nu_1\frac{\cos\theta}{r}\vartheta. \quad (26)$$

From the equation of projections of all forces on the direction of the normal, taking into account

$$N_1=Q_z\sin\theta+Q_r\cos\theta,$$

$$Q_1=-Q_z\cos\theta+Q_r\sin\theta,$$

we obtained:

$$\frac{1}{r}\frac{d}{ds}\left[\left(-Q_z\cos\theta+Q_r\sin\theta\right)r\right]-$$
$$-\frac{Q_z\sin\theta}{R_1}-\frac{Q_r\cos\theta}{R_2}-$$
$$-\frac{\nu_2}{R_2}\left(Q_z\sin\theta+Q_r\cos\theta\right)-$$
$$-\frac{E_2h}{R_2}\frac{u_r}{r}+q_n=0. \quad (27)$$

Since

$$\frac{1}{R_2}=\frac{\sin\theta}{r},$$

and

$$\frac{d\theta}{ds}=\frac{1}{R_1},\ \ N_2=\nu_2N_1+E_2h\varepsilon_2,$$

then you can convert:

$$\frac{N_2}{R_2}=\frac{\nu_2N_1+E_2h\frac{u_r}{r}}{R_2}=$$
$$=\frac{\nu_2}{R_2}\left(Q_z\sin\theta+Q_r\cos\theta\right)+\frac{E_2h}{R_2}\frac{u_r}{r}. \quad (28)$$

Knowing that

$$\frac{d}{ds}=\left(rQ_z\right)=\left(q_n\cos\theta-q_1\sin\theta\right)r, \quad (29)$$

$$\frac{dr}{ds}=\cos\theta,$$

$$-\left(q_n\cos\theta-q_1\sin\theta\right)\cos\theta+q_n=q_1\sin\theta,$$

then:

$$-\frac{1}{r}\frac{d\left(Q_zr\right)}{ds}\cos\theta+\frac{1}{r}\frac{d\left(Q_zr\right)}{ds}\sin\theta+$$
$$+Q_z\sin\theta\frac{d\theta}{ds}+Q_r\cos\theta\frac{d\theta}{ds}-$$
$$-Q_z\sin\theta\frac{d\theta}{ds}-Q_r\cos\theta\frac{d\theta}{ds}-\frac{\nu_2\sin^2\theta}{r}Q_z-$$
$$-\frac{\nu_2\cos\theta\sin\theta}{r}Q_r\frac{E_2h\sin\theta}{r^2}u_r+q_n=0. \quad (30)$$

$$\frac{dQ_r}{ds}=\frac{E_2h}{r^2}u_r+\frac{\nu_2\cos\theta}{r}Q_r+$$
$$+\frac{\nu_2\sin^2\theta}{r}Q_z-\frac{Q_r}{r}\cos\theta-q_r, \quad (31)$$

$$\frac{dQ_r}{ds}=\frac{E_2h}{r^2}u_r+\frac{(1-\nu_2)\cos\theta}{r}Q_r+\frac{\nu_2\sin^2\theta}{r}Q_z-q_r. \quad (32)$$

From the condition

$$\frac{d}{ds}\left(rQ_z\right)=\left(q_n\cos\theta-q_1\sin\theta\right)r,$$

taking into account $q_z=-q_n\cos\theta+q_1\sin\theta$:

$$r\frac{dQ_z}{ds}+Q_z\frac{dr}{ds}=r\frac{dQ_z}{ds}+Q_z\cos\theta=-q_z\cdot r\Rightarrow$$
$$\Rightarrow\frac{dQ_z}{ds}=-\frac{\cos\theta}{r}Q_z-q_z\cdot r. \quad (33)$$

From the equation of projections of all forces on the direction of the normal, taking into account

$$M_2=\nu_2M_1+\frac{E_2h^3}{12}\frac{\cos\theta}{r}\vartheta,$$

we obtained:

$$\frac{1}{r}\frac{d}{ds}\left(M_1r\right)-M_2\frac{\cos\theta}{r}-Q_1=0,$$

$$\frac{1}{r}r\frac{dM_1}{ds}+\frac{1}{r}M_1\frac{dr}{ds}-M_2\frac{\cos\theta}{r}-Q_1=0,$$

$$\frac{dM_1}{ds}+\frac{M_1}{r}\frac{dr}{ds}-\nu_2M_1\frac{\cos\theta}{r}-$$
$$-\frac{E_2h^3}{12}\frac{\cos\theta}{r}\vartheta\frac{\cos\theta}{r}-Q_1=0,$$

$$\frac{dM_1}{ds}+\frac{M_1}{r}\cos\theta-\nu_2M_1\frac{\cos\theta}{r}-$$
$$-\frac{E_2h^3}{12}\frac{\cos\theta}{r}\vartheta\frac{\cos\theta}{r}-Q_1=0, \quad (34)$$

$$\frac{dM_1}{ds}+M_1\left(\frac{\cos\theta}{r}--\nu_2\frac{\cos\theta}{r}\right)-$$
$$-\frac{E_2h^3\vartheta}{12r^2}\cos^2\theta-Q_1=0,$$

$$\frac{dM_1}{ds}+\frac{(1-\nu_2)\cos\theta}{r}M_1-\frac{E_2h^3\vartheta}{12r^2}\cos^2\theta-Q_1=0,$$

$$\frac{dM_1}{ds}+\frac{(1-\nu_2)\cos\theta}{r}M_1-$$
$$-\frac{E_2h^3\vartheta}{12r^2}\cos^2\theta+Q_z\cos\theta-Q_r\sin\theta=0,$$

$$\frac{dM_1}{ds}=\frac{E_2h^3\vartheta}{12r^2}\cos^2\theta+$$
$$+Q_r\sin\theta-Q_z\cos\theta-\frac{(1-\nu_2)\cos\theta}{r}M_1.$$

Thus, the desired system of differential equations is as follows:

$$\frac{du_r}{ds}=\frac{1-\nu_1\nu_2}{E_1h}Q_z\sin\theta\cos\theta+\frac{1-\nu_1\nu_2}{E_1h}Q_r\cos^2\theta-$$
$$-\nu_1\frac{E_2}{E_1}\cos\theta\frac{u_r}{r}-\vartheta\sin\theta,$$

$$\frac{du_z}{ds}=\frac{1-\nu_1\nu_2}{E_1h}Q_z\sin^2\theta+\frac{1-\nu_1\nu_2}{E_1h}Q_r\sin\theta\cos^2\theta-$$
$$-\nu_1\frac{E_2}{E_1}\sin\theta\frac{u_r}{r}+\vartheta\cos\theta,$$

$$\frac{d\vartheta}{ds}=\frac{12\left(1-\nu_1\nu_2\right)}{E_1h^3}M_1-\frac{E_2}{E_1}\nu_1\frac{\cos\theta}{r}\vartheta,$$

$$\frac{dQ_r}{ds}=\frac{E_2h}{r^2}u_r-\frac{\left(1-\nu_2\right)\cos\theta}{r}Q_r+\frac{\nu_2\sin\theta}{r}Q_z-q_r, \qquad (35)$$

$$\frac{dQ_z}{ds}=-\frac{\cos\theta}{r}Q_z-q_z\cdot r,$$

$$\frac{dM_1}{ds}=\frac{E_2h^3\vartheta}{12r^2}\cos^2\theta+Q_r\sin\theta-$$

$$-Q_z\cos\theta-\frac{\left(1-\nu_2\right)\cos\theta}{r}M_1.$$

As a result of theoretical transformations, a system of ordinary differential equations for determining internal forces and displacements in corrugated shell elements made of composite materials was obtained (35).

5. 3. Reducing a system of equations to a dimensionless form and determining the state vector

For numerical integration (35), the method of initial parameters is used. This method is not always applicable because of the fast-growing and fast-decreasing solutions, i.e., because of the so-called "flattening" of the system of solution vectors. To avoid this, the method of running and orthogonalizing the results at the intermediate points of division of the integration segment, which is proposed in [20], helps. According to it, the integration segment is divided into a number of intermediate segments so that numerical integration of the system of equations (35) within any intermediate section is possible. The number of partition points of the integration segment is set empirically. The system of vectors in the second and subsequent sections is solved with the initial parameters, which came out as a result of the integration of the equations of the previous integration segment.

The dependence $U=Uz(p)$ is the static characteristic of the elastic element of interest to us. Varying the geometric dimensions and methods of reinforcement, we obtain various components of the state vector at all points of interest of the middle surface. The stresses in the mutually perpendicular sections, one of which lies in a plane parallel to the meridional plane, the other in a plane perpendicular to the middle surface of SEE, are determined from formulas:

$$\sigma_1=N_1/h\pm6M_1/h^2;\ \ \sigma_2=N_2/h\pm6M_2/h^2, \qquad (36)$$

where σ_1, N_1, M_1 are, respectively, the stress, the normal force, the bending moment in a cross-section perpendicular to the middle surface, σ_2, N_2, M_2 are similar values in the cross-section parallel to the meridional plane. In (36), the plus sign is for stresses on a stretched surface, and the minus sign is for stresses on the compressed surface. The stress in the cross-section parallel to the middle surface is neglected according to the accepted Kirchhoff-Love conjecture. The force factors included in equation (36) are determined through the components of the state vector according to the formulas:

$$N_1=Q_r\cos\theta+Q_z\sin\theta,$$

$$N_2=\nu_2N_1+E_2hu_r/r,$$

$$M_1=M_1, \qquad (37)$$

$$M_2=\nu_2M_1+E_2h^3\cos\theta\cdot\nu/\left(12r\right).$$

The equivalent stress is determined by energy theory:

$$\sigma_{equiv}=\sqrt{\sigma_1^2+\sigma_2^2-\sigma_1\sigma_2}. \qquad (38)$$

Strength testing is carried out by force:

$$\sigma_{equiv}\prec\left[\sigma\right]=\sigma_y/n_y, \qquad (39)$$

where $[\sigma]$ is the allowable stress; σ_y is the yield strength at stretching or compression; n_y is the yield factor.

As a result of the calculation, 15 components of the state vector are obtained:

1. Axial displacement – u_z.
2. Radial displacement – u_r.
3. Transverse force – Q_r.
4. Transverse force – Q_z.
5. Bending moment – M_1.
6. Bending moment – M_2.
7. Longitudinal force – N_1.
8. Longitudinal force – N_2.
9. Tensile stress – $\sigma_1^t=N_1/h$.
10. Bending stresses $\sigma_1^b=6M_1/h^2$.
11. Stresses – $\sigma_1=\sigma_1^t\pm\sigma_1^b$.
12. Tensile stresses $\sigma_2^t=N_2/h$.
13. Bending stresses $\sigma_2^b=6M_1/h^2$.
14. Stresses – $\sigma_2=\sigma_2^t\pm\sigma_2^b$.
15. Equivalent stresses $\sigma_{equiv}=\sqrt{\sigma_1^2+\sigma_2^2-\sigma_1\sigma_2}$.

5. 4. Determination of displacements, forces, and stresses in corrugated elastic elements

As a test example, an isotropic shell with the following physical and mechanical characteristics was calculated: E=100,000 MPa; ν=0.33. According to the proposed calculation method, the following results were obtained.

At a pressure of 0.01 MPa according to the Godunov method, the deflection in the center of the membrane is 0.128 mm (in the present work and in the experiment described in [2] – 0.127 mm).

Fig. 6 shows the diagrams of normal stresses σ_1 during bending and stretching, calculated from the results of this study and from the results of the test example.

Fig. 7 shows the diagrams of normal stresses σ_2 during bending and stretching, calculated from the results of this study and from the results of the test example.

The maximum bending stress occurs at the outer contour of the membrane, where it (according to the Godunov method) is 59 MPa, (according to the algorithm proposed in this work, 58.84 MPa). The stress diagrams are completely identical in nature, and the difference in numbers does not exceed 0.27 % (Fig. 6, 7).

Fig. 8 shows the elastic characteristics of the element, determined from various theoretical and experimental data.

Fig. 8 shows the elastic characteristics of the shell element, built as a result of analytical calculations obtained in this work (3), according to the analytical calculations proposed in [1] – (1), [2] – (2), and experimental data obtained in [1] – (3). As can be seen from Fig. 8, the results of the proposed calculation method coincide with the experimental data and therefore, accurately reflect the behavior of the shell under load. It can be concluded that the calculation method, as well as the program implementing it, are accurate enough to be used in practice.

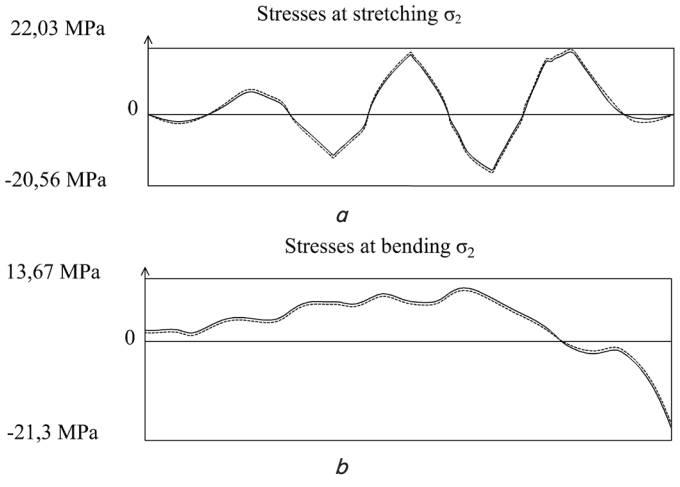

Fig. 6. Normal stress σ_2 diagrams when stretching and bending: *a* — when stretching: _____ — test, ... — calculation; *b* — when bending: _____ — test, ... — calculation

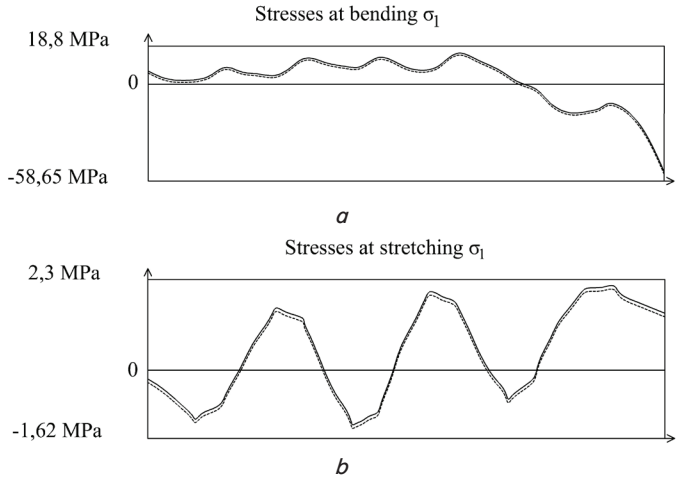

Fig. 7. Normal stress σ_1 diagrams when stretching and bending: *a* — when bending: _____ — test, ... — calculation; *b* — when bending: _____ — test, ... — calculation

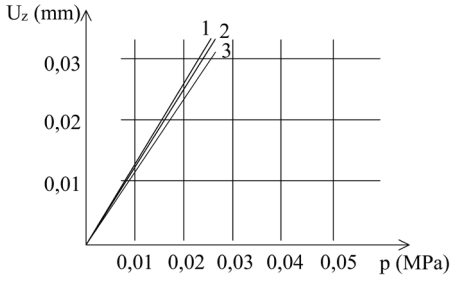

Fig. 8. Elastic characteristics of the shell element: 1 — analytical calculation [1]; 2 — according to the Godunov method; 3 — according to the results of this study

Fig. 9 shows the diagrams of the vertical displacements U_z, the radial displacements U_r, the transverse forces Q_r, the transverse forces Q_z, the bending moments M_1.

These forces are defined for three combinations of fiber and matrix in radial reinforcement. The softest matrix (magnesium) and the stiffest fiber (boron) are combination 1, the stiffest "matrix" (copper, medium stiffness fiber (steel) is combination 2, medium stiffness values of the matrix and fibers (aluminum-steel) are combination 3. The geometric dimensions of all shells are the same, the load p=0.01 MPa. Radial displacements are, respectively, 0.006 mm, 0.0035 mm, 0.005 mm.

The character of the diagram of the transverse forces Q_z resembles the profile of the shell, but the maximum values of the transverse forces are near the hollows of the shell, and the minimum values are vice versa, near the vertices. Values of maximum forces for combinations a, b, c (respectively): 0.4 kN/m; 0.467; 0.446. The minimum values of the transverse forces Q_z in all cases are the same: 0.0095 kN/m, and the maximum 0.107 kN/m; 0.12 kN/m; 0.11 kN/m – for options a, b, c, respectively.

The diagram of the bending moments M_1 resembles a sine wave in nature, only with a period half that of the shell. On the "troughs" and "vertices" of the shell, the moment values are the smallest in their period, the maxima of moments fall on the "zero" points of the shell. Starting the last half-wave of the sine wave of the shell, the values of the moment M_1 fall sharply, which can be explained by the presence of a boundary effect. At the base of the rigid center of the shell, where the largest concentration of reinforcing fibers is, the influence of the value of the modulus of elasticity of the fiber is manifested: when combined fibers and matrices, i.e., at the most "rigid" fiber, the value of the moment M_1 at the rigid center significantly exceeds similar moment values for other combinations of fiber and matrix:

a) M_{1max}=0.43 kN/m;
b) M_{1max}=0.16 kN/m;
c) M_{1max}=0.158 kN/m.

The values of non-moments at the outer edge of the shell, the concentration of fibers has a much smaller effect on the stiffness, close to each other:

a) –0.45 kN/m;
b) –0.487 kN/m;
c) –0.47 kN/m.

Since the matrix material has a much smaller modulus of elasticity compared to fiber, and when the membrane is loaded, the length of the threads remains practically unchanged, the change in the shape of the membrane under load is associated with shear deformations in the matrix. Therefore, the calculation was made for each combination of fiber and matrix twice: without taking into account the shift and taking into account it.

Fig. 10 shows the elastic characteristics of the shell element at the radial arrangement of reinforcing fibers for their different concentrations: ψ=0.785, ψ=0.81, ψ=0.906.

Fig. 10, 11 show the elastic characteristics of the element depending on the concentration of the reinforcing fiber during radial and ring reinforcement. Obviously, the greater the fiber concentration (in both cases of reinforcement), the more rigid the characteristic.

Fig. 12 shows elastic characteristics at different shell thicknesses. Reinforcement in all cases is radial.

Fig. 13 shows elastic characteristics at different shell thicknesses. Reinforcement in all cases is circular.

Fig. 12, 13 demonstrate that the thickness of the shell significantly affects the elastic characteristic: the greater the thickness of the shell, the stiffer it is, and therefore less sensitive. This dependence persists for both radial and ring reinforcement, although the shells are stiffer with ring reinforcement than with radial reinforcement. With a thickness of the shell h=0.05 mm, radial reinforcement gives a rapid increase in displacement with a slight increase in load, which

violates the gentle linearity of the elastic characteristic, with ring reinforcement, almost the same thing happens. At thickness h=0.22 mm, radial reinforcement retains the linearity of the characteristic up to p=0.015 MPa, ring – up to 0.05 MPa, with a thickness of 0.45 mm, radial reinforcement gives a linear characteristic up to p=0.06 MPa, ring – with an unlimited p. At a minimum thickness, the radially reinforced shell is much more stressed than the ring; with increasing thickness, this difference disappears.

Fig. 14 shows the elastic characteristics of the element in various combinations of fiber and matrix without taking into account shear. Reinforcement in all cases is orthogonal.

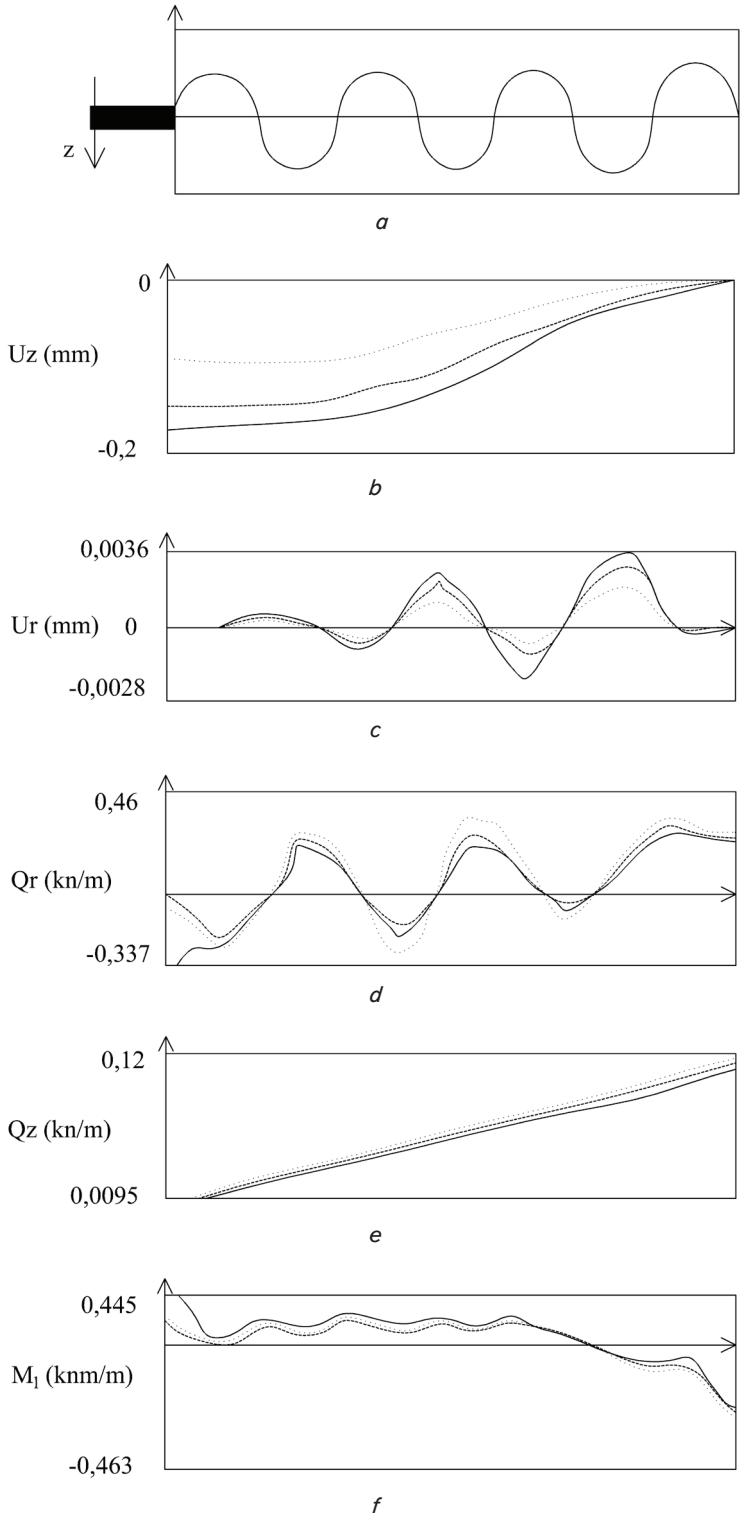

Fig. 9. Force diagrams: *a* – estimation scheme, *b* – diagram of vertical displacements U_z; *c* – radial displacement diagram U_r; *d* – diagram of the transverse radial forces Q_r; *e* – diagram of transverse forces Q_z; *f* – diagram of bending moments M_1; _____ – combination 1; ····· – combination 2; -------- – combination 3

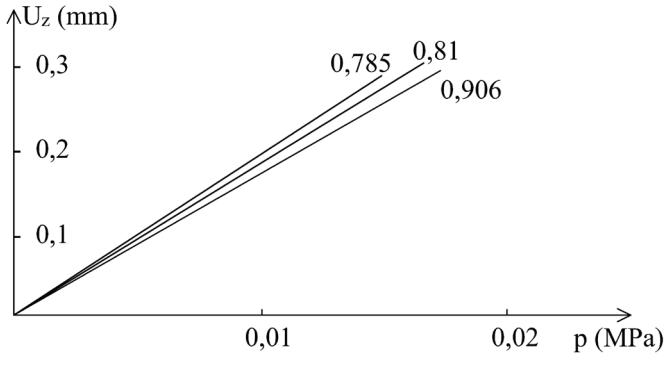

Fig. 10. Elastic characteristics in the radial arrangement of fibers depending on the concentration of reinforcing fibers

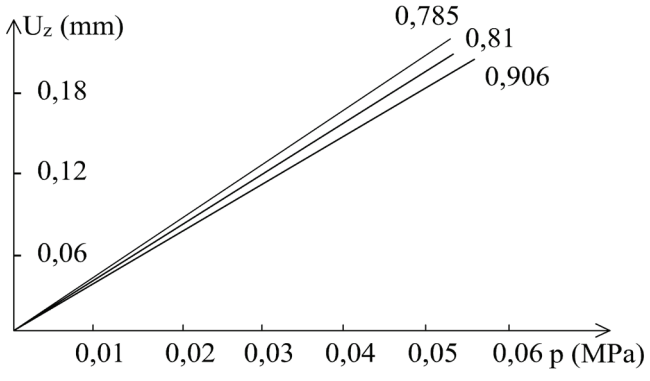

Fig. 11. Elastic characteristics in the ring arrangement of fibers at different concentrations: ψ=0.785; ψ=0.81; ψ=0.906

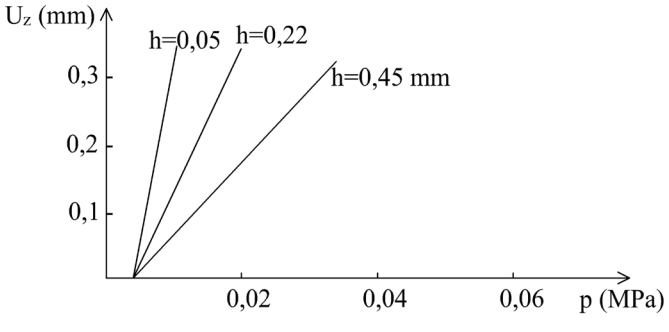

Fig. 12. Elastic characteristics at different thicknesses of the shell (radial reinforcement)

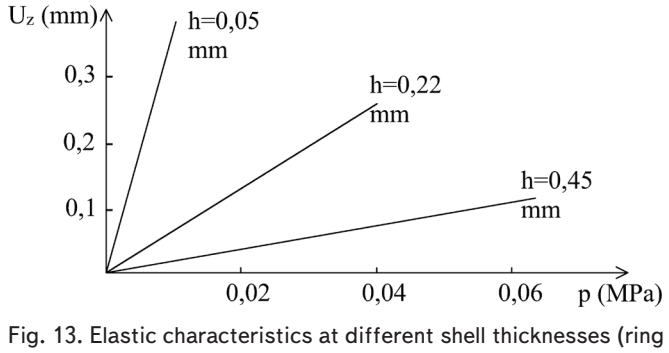

Fig. 13. Elastic characteristics at different shell thicknesses (ring reinforcement)

Fig. 15 shows the elastic characteristics of the element in various combinations of fiber and matrix without taking into account the shift and taking into account the shift. Reinforcement in all cases is orthogonal.

The plots in Fig. 14 show (straight lines 5, 3, 1) that the shells with the stiffest fiber (boron) have the greatest stiffness, and therefore the least sensitivity. The influence of the matrix in them is weaker, although the shells with a "softer" matrix are less rigid. The next two characteristics are straight lines 2 and 4 - belong to the elements where steel was used as a fiber. These two straight lines are located very close to each other, that is, the matrix material practically does not create a difference in the stress-stressed state. This can be seen in the values of equivalent stresses in the second combination of fibers of the matrix σ_{equiv}=57.3 MPa at p=0.01 MPa, and at the fourth combination at the same pressure σ_{equiv}=57.34 MPa.

The sixth combination of fiber and matrix provides a fairly "soft" sensitive shell with σ_{eq}=56.6 MPa at p=0.01 MPa. The linearity of the elastic characteristic is preserved with the third and fifth variants of the fiber and matrix combinations at p=0.047 MPa, with the first to p=0.04 MPa, with the second and fourth – up to p=0.032 MPa, with the sixth – up to p=0.02 MPa.

When analyzing the plots shown in Figs. 14, 15, it can be seen that in the first and second variants, combinations of fiber and shear matrix practically do not occur. In the first variant, at p=0.01 MPa, the displacement of the rigid center without taking into account the shift is 0.068 mm, taking into account the shift – 0.063 mm, σ_{equiv}=53.6 MPa (excluding shift), σ_{eq}=52.6 MPa (taking into account the shift).

In the second option, without taking into account the shift:

U_z=0.084 mm, σ_{equiv}=57.34 MPa at p=0.01 MPa;

taking into account the shift

U_z=0.083 mm, σ_{equiv}=57.26 MPa.

At the same pressure, it is obvious that in the first case, very rigid boron fibers "hold" the malleable matrix, and in the second, a fairly rigid matrix resists shear well. In the remaining four cases, the effect of shear is already great: malleable matrices resist weakly, and not very "rigid" fibers cannot provide the overall stiffness of the element. Moreover, the "softer" the matrix, the greater the effect of the shift, the greater the difference in elastic characteristics and stresses.

Fig. 16 shows the obtained elastic characteristics with various combinations of radial and ring fiber in the case of orthogonal reinforcement.

The matrix is magnesium. The most rigid characteristic is in the shell with reinforcing fibers radial from aluminum, ring - from boron. Here, the linearity is maintained until the pressure load is 0.045 MPa, and the σ_{eq}=58.72 MPa at p=0.01 MPa. The characteristic with the first combination of radial and ring fibers is the "softest", the linearity is maintained until the pressure reaches 0.017 MPa. The most rigid characteristic is in the shell with reinforcing radial fibers made of aluminum, ring – from boron. Here the linearity is preserved until the pressure is loaded with a pressure of 0.045 MPa, and σ_{equiv}=58.72 MPa at p=0.01 MPa. Characteristic with the first combination of radial and ring fibers – the "softest" linearity is maintained until a pressure of 0.017 MPa is reached, σ_{eq}=56.6 MPa at p=0.01 MPa. From a comparison

of these three characteristics, it can be concluded that ring reinforcement gives greater rigidity to the shell than radial.

Fig. 17 shows the elastic characteristics in various types of reinforcement.

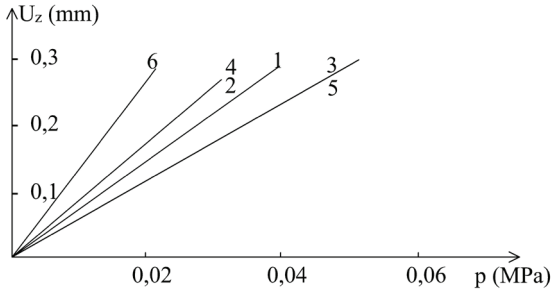

Fig. 14. Elastic characteristics for various combinations of fiber and matrix (orthogonal reinforcement) without taking into account shear: 1 — boron-magnesium; 2 — steel-copper; 3 — boron-copper; 4 — steel-aluminum; 5 — boron-aluminum; 6 — aluminum-magnesium

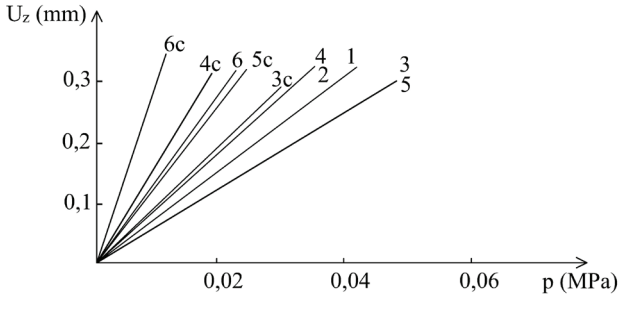

Fig. 15. Elastic characteristics for various combinations of fiber and matrix (orthogonal reinforcement) without shear and taking into account shear: 1 — boron-magnesium; 2 — steel-copper; 3 — boron-copper; 4 — steel-aluminum; 5 — boron-aluminum; 6 — aluminum-magnesium

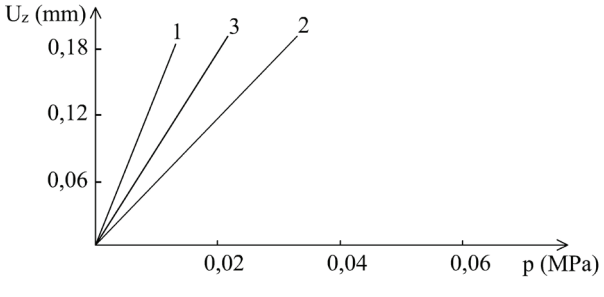

Fig. 16. Elastic characteristics with various combinations of radial and ring fiber: 1 — boron-aluminum; 2 — aluminum-boron; 3 — steel-steel

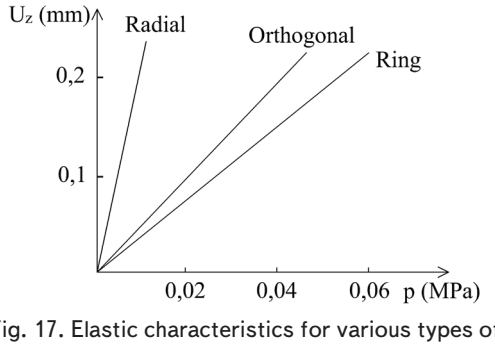

Fig. 17. Elastic characteristics for various types of reinforcement

The most "rigid" shell is with ring reinforcement, the linearity of the characteristic is preserved until the pressure load is 0.06 MPa, while with radial reinforcement up to 0.013 MPa "Intermediate" is orthogonal reinforcement: here the linearity is preserved up to 0.035 MPa.

6. Discussion of results of applying the methodology for determining the static characteristics of elastic shell elements

Estimation schemes of deformed (Fig. 1) and undeformed shells (Fig. 2) were drawn up. Various combinations of materials for the manufacture of shell elements are presented (Tables 2, 3). After mathematical transformations of the equilibrium equations and determination of the magnitude of the mechanical characteristics of materials (1) to (5), equations (35) were built. To solve them, a program for calculating efforts and displacements has been compiled. The reliability of the theoretical results is confirmed by experimental data [1] conducted for isotropic shells. This is also confirmed by test calculations, the results of which are reflected in Fig. 6–8. The reliability of the results obtained is explained by the correctly chosen estimation scheme of the shell element and the rational system of differential equations (35). The peculiarity of the proposed method is that it takes into account both the complex geometry of the shell and uneven reinforcement. Studies were carried out under the condition of linearity of the elastic characteristic. In the subsequent developments, it is proposed to increase the class of studied problems by determining nonlinear elastic characteristics. The system of equations (35) does not allow such an analysis to be made. As a shell material, a scheme of composite material "metal on metal" is used. Difficulties may arise when implementing the results of the technical plan study: the technology for the manufacture of such shell elements has not yet been sufficiently developed.

Based on the results of calculations of internal forces and displacements, recommendations can be made for the design of corrugated shell elements from composite materials. To obtain linear elastic characteristics, you can use:

a) radially reinforced shells with a rigid matrix (permissible pressure – 0.035 MPa) or soft (permissible pressure 0.01 MPa);

b) ring-reinforced boron fibers – permissible pressure of 0.06 MPa; steel fibers – permissible pressure 0.035 MPa; aluminum fibers – permissible pressure 0.015 MPa;

c) orthogonally reinforced shells.

Recommendations:

1. In shell elements with ring reinforcement, the decisive role is played by the material of the reinforcing fiber, in contrast to radially reinforced elements, where the matrix material is decisive.

2. Depending on the choice of material, the displacement fibers of the center of the shell have a significant variation in values at the same pressure: from 0.03 mm (boron) to 0.18 mm (aluminum).

3. To obtain a linear elastic characteristic when using boron fibers in the case of ring reinforcement, the shell can be loaded with pressure up to 0.06 MPa. If the fibers are made of steel, the pressure should not exceed 0.035 MPa, and with aluminum fibers not more than 0.015 MPa. Otherwise, linear theory is unacceptable.

The results of the study determine the maximum possible pressure values to obtain linear elastic characteristics. If these values are exceeded, the nature of the dependences has not been studied. It is assumed that the linearity of the elastic characteristic above the calculated pressure values will not be observed. There is a need to derive a new system of equations taking into account nonlinearity. This is undoubtedly a very time-consuming task that can be solved in future studies. These conclusions can be attributed to the shortcomings of the proposed method. This is also the goal of future research. The complexity of the task will lie in mathematical calculations (taking into account the nonlinearity of several types), and in the manufacture of elastic shells with a complex meridian shape and uneven reinforcement. Metal-to-metal reinforcement has not yet found much application in technology, mainly composites made of plastic materials are used. This is another factor that complicates research. Although the composite "metal on metal" can reduce the own weight of the element. This, of course, is an important aspect of the operation of the entire structure and will lead to savings in both the material and the cost of the elements.

7. Conclusions

1. An estimation scheme of an elastic element as a shell of rotation during deformation is drawn up and equilibrium equations are derived. A feature of this scheme is the accounting of the anisotropy of the structure caused by uneven reinforcement, as well as the possibility of taking into account the geometric and physical parameters of the shell at each point. When solving these equations, it is possible to obtain static characteristics not only of isotropic structures but also to combine various materials in the structure, both matrices and fibers.

2. Equations for determining displacements and forces in corrugated shell elastic elements are derived. A feature of these equations is the consideration of the mechanical and geometric parameters of the shell, which are variable values at each point of the section. This is due to the peculiarity of the design of the shell element, caused by uneven reinforcement.

3. The system of equations is reduced to a dimensionless form and the state vector of the system is obtained to compile the algorithm of the computational program for the PC.

4. Displacements, forces, and stresses in corrugated elastic elements have been determined. Based on the results, elastic characteristics of shell elements are constructed under various combinations of matrix and fiber materials, at different geometric parameters. Recommendations to designers for the manufacture of shell elements with specified characteristics of rigidity and sensitivity are given.

Conflicts of interest

The authors declare that they have no conflicts of interest in relation to the current study, including financial, personal, authorship, or any other, that could affect the study and the results reported in this paper.

Funding

The study was conducted without financial support.

Data availability

All data are available in the main text of the manuscript.

References

1. Andreeva, L. E. (1962). Uprugie elementy priborov. Moscow: Mashgiz, 456.
2. Alfutov, N. A., Zinov'ev, P. A., Popov, B. G. (1984). Raschet mnogosloynyh plastin i obolochek iz kompozitsionnyh materialov. Moscow: Mashinostroenie, 264.
3. Shimyrbaev, M. K. (1992). Utochnennye metody opredeleniya uprugih postoyannyh odnonapravlenno armirovannogo materiala. Vestnik AN RK.
4. Kurochka, K. S., Nesterenya, I. L. (2014). Raschet mnogosloynyh osesimmetrichnyh obolochek metodom konechnyh elementov. Informatsionnye tekhnologii i sistemy 2014 (ITS 2014): materialy mezhdunarodnoy nauchnoy konferentsii. Minsk, 214–215. Available at: https://libeldoc.bsuir.by/handle/123456789/2008
5. Golova, T. A., Andreeva, N. V. (2019). Analysis of methods of calculation of layered plates and shells for the calculation of multilayer structures. The Eurasian Scientific Journal, 5 (11).
6. Bazhenov, V. A., Solovei, N. A., Krivenko, O. P., Mishchenko, O. A. (2014). Modeling of nonlinear deformation and buckling of elastic inhomogeneities shells. Stroitel'naya mekhanika inzhenernyh konstruktsiy i sooruzheniy, 5, 14–33.
7. Kairov A. S., Vlasov O. I., Latanskaya L. A. (2017). Free vibrations of constructional non-homogeneous multilayer orthotropic composite cylindrical shells. Visnik Zaporiz′kogo nacional′nogo universitetu. Fiziko-matematicni nauki, 2, 57–65.
8. San'kov, P., Tkach, N., Voziian, K., Lukianenko, V. (2016). Composite building materials and products. International scientific journal, 4 (1), 80–82. Available at: http://nbuv.gov.ua/UJRN/mnj_2016_4(1)__24
9. Yankovskii, A. P. (2020). The refined model of viscoelastic-plastic deformation of reinforced cylindrical shells. PNRPU Mechanics Bulletin, 1, 138–149. doi: https://doi.org/10.15593/perm.mech/2020.1.11
10. Bakulin, V. N. (2019). Posloyniy analiz napryazhenno-deformirovannogo sostoyaniya trekhsloynyh obolochek s vyrezami. Izvestiya Rossiyskoy Akademii Nauk. Mekhanika Tverdogo Tela, 2, 111–125. doi: https://doi.org/10.1134/s0572329919020028

11. Senjanović, I., Čakmak, D., Alujević, N., Ćatipović, I., Vladimir, N., Cho, D.-S. (2019). Pressure and rotation induced tensional forces of toroidal shell and their influence on natural vibrations. Mechanics Research Communications, 96, 1–6. doi: https://doi.org/10.1016/j.mechrescom.2019.02.003
12. Polyakova, I., Imambayeva, R., Aubakirova, B. (2021). Determining the dynamic characteristics of elastic shell structures. Eastern-European Journal of Enterprise Technologies, 6 (7 (114)), 43–51. doi: https://doi.org/10.15587/1729-4061.2021.245885
13. Abramczyk, J. (2021). Transformed Shell Structures Determined by Regular Networks as a Complex Material for Roofing. Materials, 14 (13), 3582. doi: https://doi.org/10.3390/ma14133582
14. Treshchev, A., Lapshina, M., Zavyalova, Y. (2021). Thermomechanical deformation of the orthotropic shell taking into account the deformation anisotropy. E3S Web of Conferences, 274, 03026. doi: https://doi.org/10.1051/e3sconf/202127403026
15. Myntiuk, V. (2021). Spectral solution to a problem on the axisymmetric nonlinear deformation of a cylindrical membrane shell due to pressure and edges convergence. Eastern-European Journal of Enterprise Technologies, 5 (7 (113)), 6–13. doi: https://doi.org/10.15587/1729-4061.2021.242372
16. Liu, Y., Zhu, R., Qin, Z., Chu, F. (2022). A comprehensive study on vibration characteristics of corrugated cylindrical shells with arbitrary boundary conditions. Engineering Structures, 269, 114818. doi: https://doi.org/10.1016/j.engstruct.2022.114818
17. Lai, M., Eugster, S. R., Reccia, E., Spagnuolo, M., Cazzani, A. (2022). Corrugated shells: An algorithm for generating double-curvature geometric surfaces for structural analysis. Thin-Walled Structures, 173, 109019. doi: https://doi.org/10.1016/j.tws.2022.109019
18. Khurukijwanich, C., Aimmanee, S. (2021). Anisotropic behaviors of helically corrugated cylindrical shells: Homogenized in-plane stiffness. Thin-Walled Structures, 160, 107378. doi: https://doi.org/10.1016/j.tws.2020.107378
19. Khurukijwanich, C., Aimmanee, S. (2021). Anisotropic behaviors of helically corrugated cylindrical shells: Stress distributions and edge effects. Thin-Walled Structures, 168, 108263. doi: https://doi.org/10.1016/j.tws.2021.108263
20. Biderman, V. L. (1977). Mekhanika tonkostennyh konstruktsiy. Moscow: Mashinostroenie, 488.